CONSOLIDATION OF CLAY IN CHANGI AIRPORT PILOT TEST

S.L. Lee* S.A. Tan* G.P. Karunaratne* and V. Choa**

SYPNOSIS

A pilot test was conducted by the Port of Singapore Authority (PSA) during the reclamation for the Changi International Airport in Singapore to study the performance of flexible drains in accelerating consolidation of the underlying marine clays, prior to the construction of the second runway, taxiway and associated turnoffs. This paper describes a post-FEM analysis to examine the behavior of different test areas with varied drain spacing, using a CAM-CLAY constitutive model and a plane strain finite element consolidation program. The effects of vertical drains were approximated by an equivalent soil with enhanced vertical permeability obtained by equating the surface settlement of the real soil with that of the equivalent soil. Soil parameters for the model were deduced from the available laboratory and field data and were calibrated to give deformation predictions consistent with field behavior. The results of the analysis show good agreement with field performance with respect to settlement, and reasonable agreement in trend with respect to pore pressures. Pore pressure profile across the surcharge width demonstrates the back pressure effect influencing the pore pressure and settlement in the drain area from the untreated reclamation which is underconsolidated, thereby reducing the consolidation of the treated area.

INTRODUCTION

A major reclamation project was undertaken by the Port of Singapore Authority from 1976 to 1978. A total of 645 hectares of land was reclaimed for the construction of the Changi International Airport in the Republic of Singapore. Soil investigation prior to the reclamation indicated that the second runway would lie partly on hard ground of sandstone and shale and partly on thick deposits of soft marine clay. The marine clay exists in depths up to about 40m below the sea bed and has been deposited mainly in deep channels. Long term settlements caused by the 6.5m hydraulic sand fill and the runway pavement load was estimated to be up to 2m. In order to minimise the problem of uneven settlement and heavy maintenance of the runway, soil treatment was necessary (Choa et al., 1979, 1981).

* Department of Civil Engineering, National University of Singapore.
** School of Civil and Structural Engineering, Nanyang Technological Institute, Singapore.

PILOT TEST AREA

A pilot test was carried out to compare the performance and feasibility of several soil improvement methods such as vertical sand drains, prefabricated flexible drains, surcharge and dynamic consolidation. Details of the pilot test are described by Choa et al., (1979). On the basis of the pilot test, a combination of Geodrains and surcharge was chosen as the appropriate method of soil treatment. Approximately 275,000 sq. m of marine clay under the runway with an average depth of 18.5m were treated.

Details of the pilot test area are shown in Fig.1. This area is situated in a typical marine clay infilled depression with new and old marine clays sandwiching a silty clay transition zone as shown in Section A-A. Numerous sand lenses in the new marine clay and large pockets of sand in the form of old river terraces exist on either side of the old marine clay depression which is underlain by cemented sand. A surcharge of 4.75m of sand was placed on 6.5m of hydraulic sand fill after the installation of drains. Geodrains were installed with three different spacings of 3.2m, 2.6m and 2.1m on square grids in areas GD1, GD2 and GD3 respectively. Section B-B shows the approximate cross section of GD3 estimated from the boring logs, together with the locations and types of instrumentation installed at the site.

FINITE ELEMENT PROGRAM

The finite element program used in this study is CON2D, developed at the University of California, Berkeley by Duncan et al., (1981). CON2D is a plane strain finite element program with a CAM-CLAY constitutive model for analysis of consolidation in earth masses. It has been used successfully to analyse consolidation in embankment dams during and after construction (Duncan et al., 1981), and in foundation soils under surface loads imposed by fills, building and oil storage tanks (D'Orazio and Duncan, 1984). The program analyses the coupled problem of deformation and fluid flow, and can be used to calculate deformations and pore pressures under undrained or fully drained conditions.

The CAM-CLAY Model in the program uses an elliptical yield surface in q-p' space, centred on the hydrostatic axis and an associative flow rule to describe plastic deformations. The parameters describing the yield surface are p'_c, the effective isotropic preconsolidation pressure, and M, the slope of the critical state
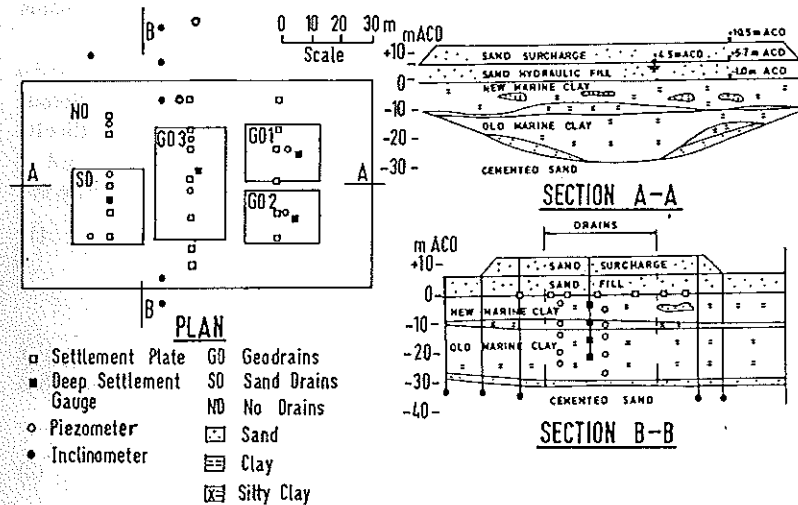
Fig. 1 Pilot test area (GD1, GD2, GD3)

line (failure surface) connecting the peak point on the yield ellipse with the origin of the q-p' space. The magnitude of the plastic strains is based on λ, the slope of the isotropic virgin consolidation curve in a void ratio-natural logarithm stress space. Elastic deformations are described by κ, the slope of the rebound curve in a void ratio-natural logarithm stress space, and the Poisson's ratio, v. Anisotropic permeability is incorporated in the program by specifying different horizontal and vertical coefficients of permeability.

EQUIVALENT VERTICAL PERMEABILITY MODEL FOR VERTICAL DRAINS

The consolidation process in soils, of low permeability accelerated by vertical drains, is usually analysed using Barron's (1948) solution or other methods (Hansbo, 1981). To perform a plane strain analysis, it is assumed that a soil with vertical drains can be approximated by an equivalent homogeneous soil whose compressibility is identical to the real soil, but the coefficient of vertical permeability is enhanced to reflect the presence of vertical drains. The equivalent vertical permeability of the soil is obtained by equating the average degree of consolidation of the real soil to the average degree of consolidation of the

4

5

equivalent soil. The coefficient of permeability in the horizontal direction remains unchanged.

The average degree of consolidation $\bar{U}_v$ for one-dimensional consolidation of a soil with maximum drainage path h can be expressed approximately (Scott, 1963), for $c_v t/h^2 > 0.2$, by

$$\bar{U}_v = 1 - \frac{8}{\pi^2} e^{-\pi^2 c_v t/(4h^2)} \tag{1}$$

where c_v is the coefficient of consolidation for vertical flow only.

The average degree of consolidation $\bar{U}_h$ with radial flow to a central circular drain of equivalent diameter d can be expressed approximately (Hansbo, 1981) by

$$\bar{U}_h = 1 - e^{-8c_h t/(D^2 \mu_s)} \tag{2}$$

In which

$$\mu = \ln(\frac{D}{d_s}) + \frac{k_h}{k_s} \ln(\frac{d_s}{d}) - \frac{3}{4} + \pi z(2L-z)\frac{k_h}{q_w} \tag{3}$$

where d denotes diameter of vertical drain, d_s denotes diameter of smeared soil around the vertical drain, D the influence diameter of a drain, k_h the coefficient of permeability with radial (horizontal) flow, k_s the coefficient of permeability of the smeared soil, z the depth below the location of zero excess pore pressure in the drain, L the distance along the drain between the minimum and maximum pore pressure, q_w the vertical discharge capacity of the drain and $c_h = k_h c_v/k_v$, where k_v is the coefficient of permeability of the undisturbed soil in the vertical direction.

The average degree of consolidation, $\bar{U}_{vh}$ of the real soil due to the natural vertical drainage and the radial drainage to the central drain is given by (Carillo, 1942)

$$\bar{U}_{vh} = 1 - (1-\bar{U}_v)(1-U_h) \tag{4}$$

The equivalent degree of consolidation U'_v of a circular cylinder of soil installed with a central vertical drain is given by

$$\bar{U}'_v = 1 - \frac{8}{\pi^2} e^{-\pi^2 c'_v t/(4h^2)} \tag{5}$$

where $c'_v = c_v k'_v/k_v$ and k'_v is the equivalent coefficient of permeability in the vertical direction of the drained soil.

Equating U'_v and U_{vh} in Eqs. (4) and (5), it can be shown that (Choa (1986)) the equivalent vertical permeability is given by

$$k'_v = \frac{32}{\pi^2 \mu_s}(\frac{h}{D})^2 k_h + k_v \tag{6}$$

This method of modelling vertical drains in a plane-strain finite difference scheme was used by Choa (1986), Tan et al., (1987) and Karunaratne et al., (1989).

SOIL PROPERTIES AND PARAMETERS OF TEST AREA

Figure 2 shows the properties of soils in area GD3. Borehole BH219 was drilled after the reclamation but before drain installation and surcharging. Borehole BH348 was drilled at the end of the surcharging period, two years later. From the depth profiles of soil properties, it is clear that area GD3 consists of three distinct layers, a new marine clay, an old marine clay and a sandwiched transition layer of stiff clay. The boundaries of these layers are estimated as −1.5m to −9.5m for the new marine clay, −9.5m to −12.5m for the stiff clay, and −12.5m to −29.5m for the old marine clay. A similar soil profile applies to areas GD1 and GD2 as can be deduced from the logs of boreholes BH218 and BH349, made before and after surcharging, respectively. The boundaries of soil layers in areas GD1 and GD2 are estimated as −1.05m to −7.95m for the new marine clay, −7.95m to −12.45m for a stiff marine clay with sand and peat layers, and −12.45m to −20.25m for the old marine clay.

The CAM-CLAY parameters are estimated in the following way. Detailed conventional oedometer tests were performed on undisturbed samples obtained from boreholes BH218, BH219, BH348 and BH349, giving the variation of compression index, C_c and preconsolidation pressure, P_c with depth (see Fig.2). The parameter λ is estimated to be 0.8 times C_c (Duncan et al., 1981). The factor 0.8 allows for the differences in compressibility between triaxial and one-dimensional conditions. Similarly κ is estimated to be 0.8 times the recompression index, C_r. Values of K_o, the lateral earth pressure coefficient at rest, are estimated from empirical relationships such as (Alpan, 1967) where,
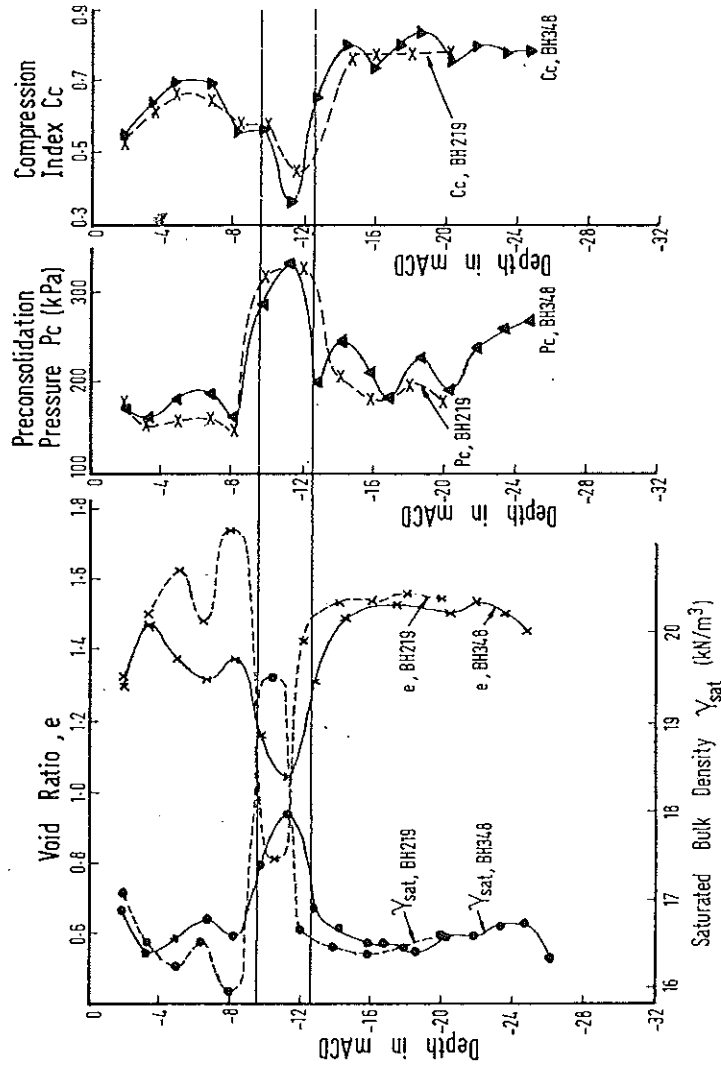
Fig. 2 Soil properties in area GD3

$K_o = 0.19 + 0.233 \log I_p$ and I_p is the plasticity index. The isotropic pre-consolidation pressure (p'_c) can be determined from the 1D preconsolidation pressure (P_c) as

$$p'_c = \frac{(1 + 2K_o)}{3} P_c \qquad (7)$$

Using values of ϕ' obtained from isotropically consolidated triaxial compression tests with pore pressure measurements, the values of the slope of the critical state line (M) can be calculated as

$$M = \frac{6 \sin\phi'}{3 - \sin\phi'} \qquad (8)$$

The Poisson's ratio, v, can be obtained from stress-strain relation of soil in confined compression as

$$v = \frac{K_o}{1 + K_o} \qquad (9)$$

The most difficult soil parameters to determine were the in-situ horizontal and vertical permeabilities. It was assumed that by the time the drain installation and surcharge was carried out, about 10 months after the reclamation, the coefficient of permeability for vertical flow had decreased to lie within a range of values similar to those obtained in the oedometer tests as shown in Fig.3. The ratio of the coefficients of permeability for horizontal flow to vertical flow was found to be about three by comparison with oedometer test results from samples cut in the horizontal and vertical directions.

The effects of vertical drains were approximated by a soil with an enhanced vertical permeability, given by Eq. (6). For the computation of the equivalent vertical permeability for drains, the coefficient of horizontal permeability of the remolded zone was assumed to be about 1×10^{-10}m/s, a value obtained from oedometer tests on remolded specimens. The other assumptions were that the drain diameter was 62mm for the Geodrains used, the equivalent diameter of the soil cylinder was 1.13 times the drain spacing in a square grid and the diameter of the smeared zone was equal to the diameter of a circle with an area twice the cross-sectional area of the mandrel, whose diameter was 170mm.

Table 1 and Table 2 show the range of values of the pertinent parameters for areas GD1, GD2 and GD3 used in the finite element analysis. The significant difference between the subsoil properties of areas GD1, GD2 and GD3 lies in the permeability of the sandwiched layer between the new and old marine clays. In
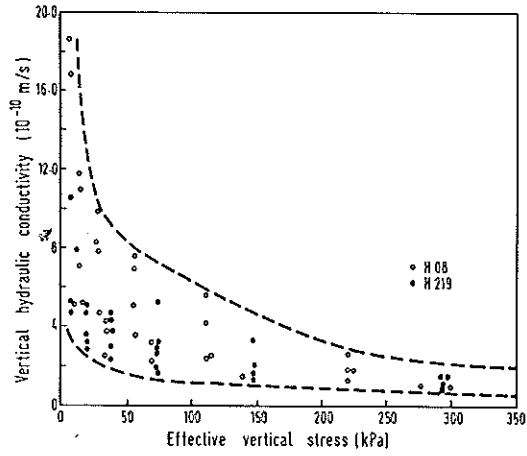
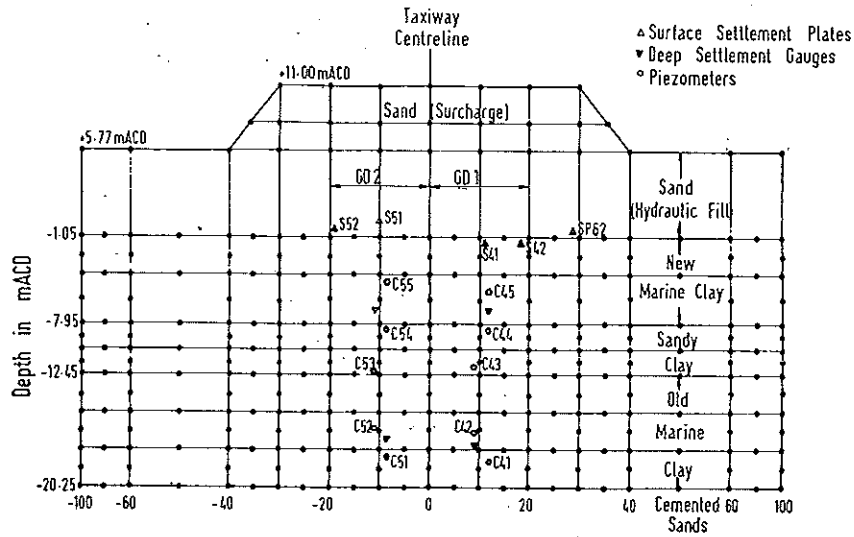Fig. 3   Vertical permeability from oedometer tests in area GD3 (from Choa, 1986)

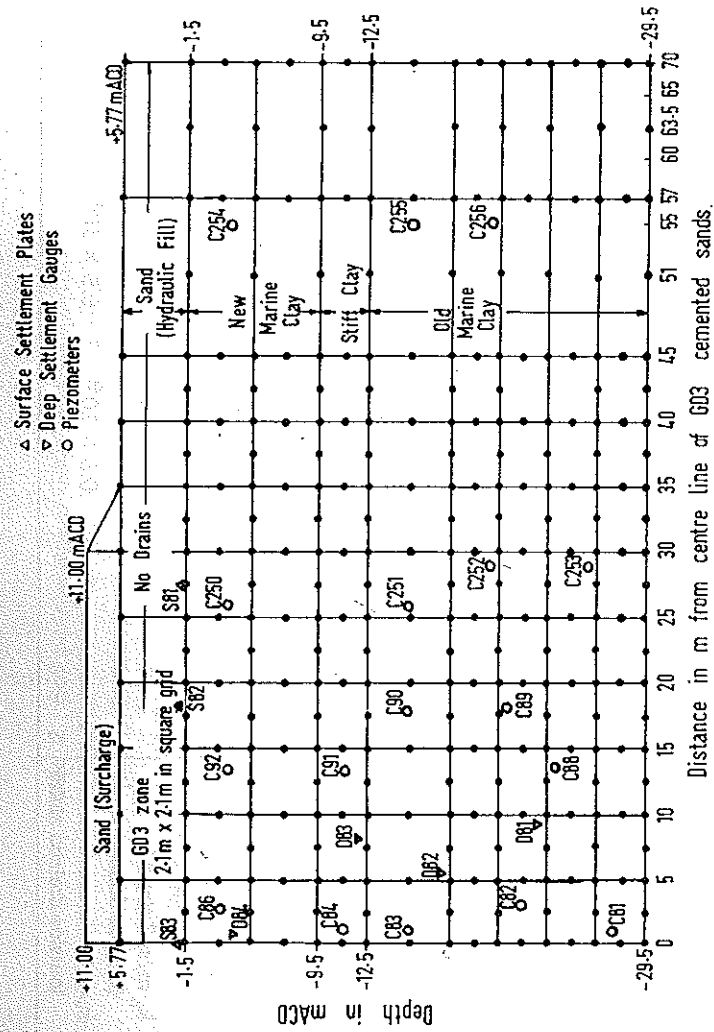Fig. 4   Finite element mesh of GD1, GD2 with instruments location

Fig. 5   Finite element mesh of GD3 with instruments location

Table 1 — Soil parameters for GD1 and GD2 Used in CON2D

Soil Properties (1)	Surcharge and Hydraulic Fill (2)	New Marine Clay (3)	Sandy Clay and Peat (4)	Old Marine Clay (5)
γ_{sat} (kN/m³)	17.0	16.3	16.9	16.6
e_0	0.8	1.4 to 1.7	1.2 to 1.4	1.5 to 1.6
Average e_0	0.8	1.6	1.3	1.55
K_0	0.5	0.59	0.54	0.59
λ	0.003	0.50	0.10	0.50
κ	0.0023	0.05	0.01	0.05
M	1.6	1.0	1.2	1.1
ν	0.33	0.37	0.37	0.37
k_h m/s (in drained zone of GD1 and GD2)		1×10^{-9}	3.3×10^{-6}	1×10^{-9}
k_v m/s (in GD1) (equiv. k in drained zone)		2.2×10^{-9}	2.2×10^{-9}	2.2×10^{-9}
(in GD2)		3.2×10^{-9}	3.2×10^{-9}	3.2×10^{-9}
k_h m/s (3 times k_v) (outside drained zone)		1.5×10^{-9}	3.3×10^{-6}	1.5×10^{-9}
k_v m/s (outside drained zone)		0.5×10^{-9}	0.5×10^{-9}	0.5×10^{-9}

Table 2 — Soil parameters of GD3 Used in CON2D

Material (1)	Surcharge and Hydraulic Fill (2)	New Marine Clay (3)	Stiff Clay (4)	Old Marine Clay (5)
γ_{sat} (kN/m³)	17.0	16.5	18.0	16.8
e_0	0.8	1.4 to 1.7	0.8 to 1.2	1.5 to 1.6
Average e_0	0.8	1.6	1.0	1.55
K_0	0.5	0.54	0.6	0.58
λ	0.003	0.52	0.38	0.62
κ	0.0023	0.052	0.038	0.062
M	1.6	1.0	1.3	1.1
ν	0.33	0.35	0.37	0.37
k_h m/s (in drained zone GD3)		1.0×10^{-9}	1.0×10^{-9}	1.0×10^{-9}
k_v m/s (equivalent k in drained zone GD3)		8.0×10^{-9}	8.0×10^{-9}	8.0×10^{-9}
k_h m/s (3 times k_v) (outside drained zone)		1.5×10^{-9}	1.5×10^{-9}	1.5×10^{-9}
k_v m/s (ave. from fig.3) (outside drained zone)		0.5×10^{-9}	0.5×10^{-9}	0.5×10^{-9}

area GD3, the stiff clay layer has a horizontal permeability of about the same order as the marine clays whereas in areas GD1 and GD2, the sandy clay layer has a horizontal permeability of three orders of magnitude higher than the marine clays as evident from the difference in the field pore pressure profiles between areas GD3, GD1 and GD2 which will be discussed later.

FINITE ELEMENT MESHES, BOUNDARY AND INITIAL CONDITIONS

Fig.4 shows the finite element mesh representing the centreline cross-section across GD1 and GD2. The full mesh was used because the drain spacing in GD1 and GD2 are different (3.2m in GD1 and 2.6m in GD2). Fig.5 shows the mesh representing only the northern half of the GD3 profile, assuming symmetry at the centreline of the area. The marine clays and the sandwiched layer were modeled using eight node isoparametric elements with pore pressure as a degree of freedom. For the hydraulic reclamation fill, 5 node isoparametric elements were used, without pore pressure degrees of freedom since fully drained behavior is assumed. Because of the high stiffness and high permeability of the cemented sands, the bottom boundary of the mesh was assumed rigid and free draining. The right hand and left hand vertical boundaries in Fig.4 and the right hand vertical boundary in Fig.5 were chosen far enough from the centreline so that horizontal deformations can be neglected.

As soil instruments were installed just prior to soil improvement works, the time rate of settlement and pore pressure dissipation at the site during and immediately after the reclamation but prior to the soil improvement works were not known. Therefore, the analysis is initialized at 10 months after the commencement of the reclamation when instruments were installed. The initial conditions were then taken as the initial void ratio profiles deduced from tests results obtained from borcholes BH218 and BH219 for areas GD1, GD2 and GD3 respectively, and initial pore pressure profiles given by the centreline piezometers C81 to C86 in area GD3 and C51 to C55 in area GD2 and C41 to C45 in area GD1. The load applied by the surcharge was modeled as two layers of fill, representing a total pressure of 70kPa.

RESULTS OF ANALYSIS AND DISCUSSION

GD1 and GD2 areas

The surface settlement profile measured by S41, S42, S51, S52 and SP62
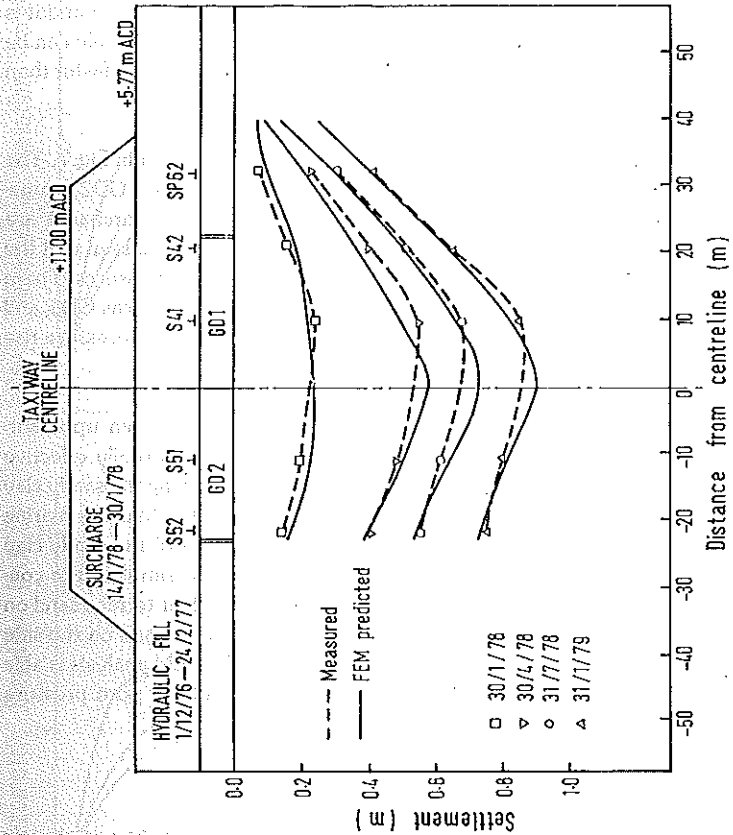
Fig. 6 Surface settlements in GD1, GD2

across GD1 and GD2 areas, immediately after surcharging and at 3 months, 6 months and one year after surcharging are shown in Fig.6. The FEM predictions of surface settlements for the corresponding periods are superimposed and it is seen that the predictions are good. The non-symmetric settlement profile can be expected as the area with the closer drain spacing (GD2) should settle faster than the area with the wider drain spacing (GD1).

The pore pressure response in areas GD1 and GD2 are shown in Fig.7. The pore pressure profile with depth for the centre of areas GD1 and GD2, immediately after surcharge and at 6 months and 12 months after surcharge are plotted together with the corresponding FEM predictions. It can be seen that the FEM predictions agree reasonably well with the measured pore pressures. There is no significant difference in pore pressure dissipation between areas GD1 and GD2 except that area GD1 seems to indicate a slightly larger pore pressure rise upon surcharging when compared with GD2.

The depression in the middle of the pore pressure profile even upon surcharging indicates that the sandy clay layer must serve as a partially effective horizontal drainage layer. This is achieved in the analysis by giving the sandy clay layer a horizontal permeability three orders of magnitude higher than the marine clays. Also at the left hand and right hand vertical boundaries of the sandy clay layer, the nodes are given a zero pore pressure condition to simulate the continuity of drainage between the sandy clay layer and the old river terrace sand on the side between the sandy clay layer and the old river terrace sand on the side slope of the marine clay valley. With these refinements, the FEM analysis is able to predict the depression in the pore pressure profiles and the pore pressure dissipation behavior as shown in Fig.7.

GD3 area

The comparison between the measured surface settlements (S81 to S83) and their FEM predictions throughout the surcharge period are shown in Fig.8. The prediction for S83, the centre vertical settlement, agrees very well with field results. The predictions for S82 and S81, the off-centre vertical settlements, are slightly underpredicted towards the end of the surcharging period.

The measured vertical settlements of the deep gauges (D81 to D84) and the FEM predictions of their response are shown in Fig.9. The predicted performance for S83 and D84 agrees very well with the measured behaviour, but the
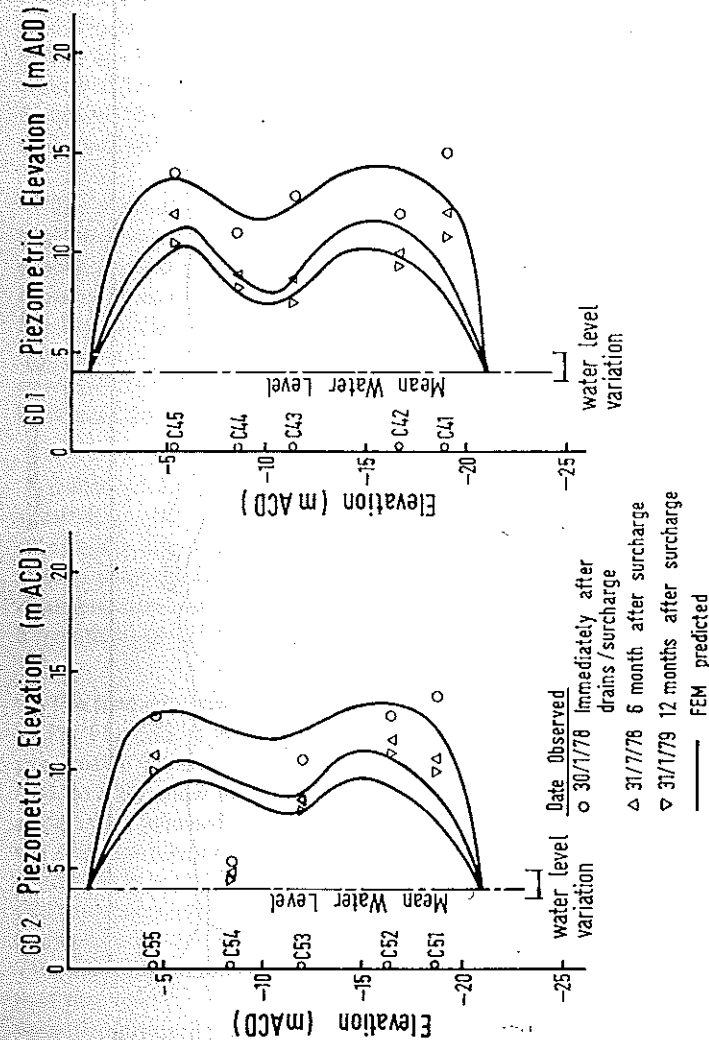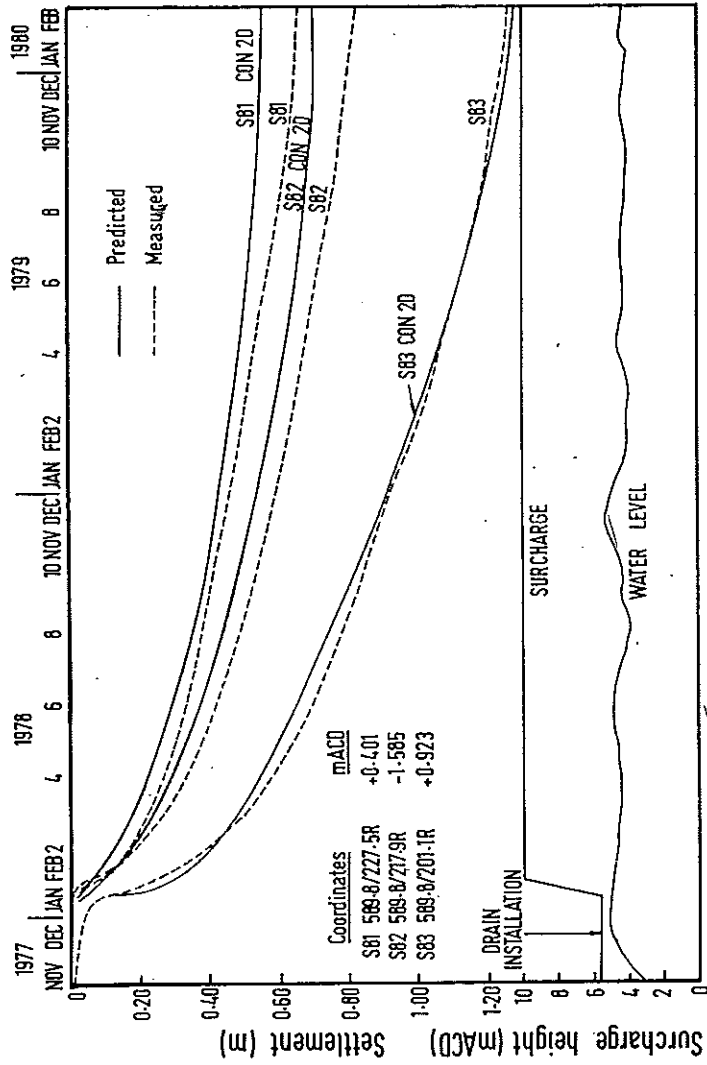
Fig. 7   Pore pressures in GD1, GD2

Fig. 8   Surface settlements in GD3

settlements of D81 to D83 are clearly underpredicted. The locations of D81 to D84 (Fig.5), indicate an overprediction of the relative settlements of the bottom half of the new marine clay layer (between D83 and D84), and an underprediction of the relative settlements of the bottom half of the old marine clay layer (between D81 and the cemented sands). However, relative settlements between D81 and D82, and D82 and D83 seem to be correctly predicted.

The measured and predicted changes in void ratios with depth between the beginning and end of the surcharge period are presented in Fig.10. Large changes in void ratios for the compressible new marine clay and relatively small changes in void ratios for the old marine clay are observed as expected. In Fig.10, the change in the predicted void ratio agrees with the observed behavior, but the void ratio changes at the bottom of the new marine clay are much overpredicted, as verified by the prediction of the relative settlements between D83 and D84 discussed previously.

Inclinometer records though available, were not included in this study because they are situated at the edge of GD3 (see Fig.1). Although absolute comparison between field and analytical results was not possible, relative magnitudes of lateral movement show consistent behaviors. FEM analysis predicted a maximum outward lateral deformation of 0.2m whereas inclinometers indicate a maximum lateral deformation of 0.1m.

The field measurements of centreline piezometers C81 to C86 are presented in Fig.11. C85 is excluded because it showed no pore pressure response, presumably being located in a sand lens in the new marine clay. Predictions for C81 to C86 show in general a rapid rise in pore pressures upon surcharge application, followed by a continuous dissipation. Piezometers located closer to the drainage boundaries showed faster dissipation of pore pressures. The field results show a higher initial pore pressure rise followed by a more rapid dissipation than predicted. With time the response of the piezometers is probably marked by the effects of drain installation and additional surcharging nearby. The difference in field behavior and prediction could be due in part to the fact that the equivalent soil model for the drained zone exhibits only rectilinear vertical and horizontal flow but not radial flow characteristics of actual vertical drains. Also the method of obtaining the equivalent permeability is based on the average degree of consolidation with respect to settlements, and hence it is expected that the analysis will not be able to predict pore pressures in the
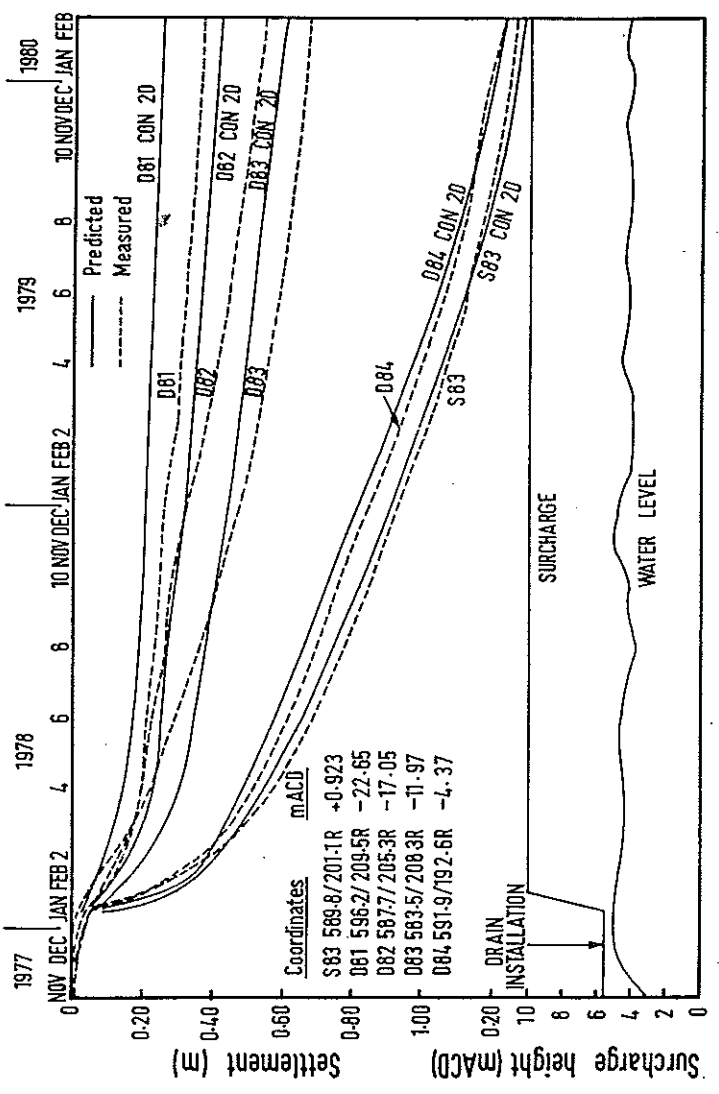
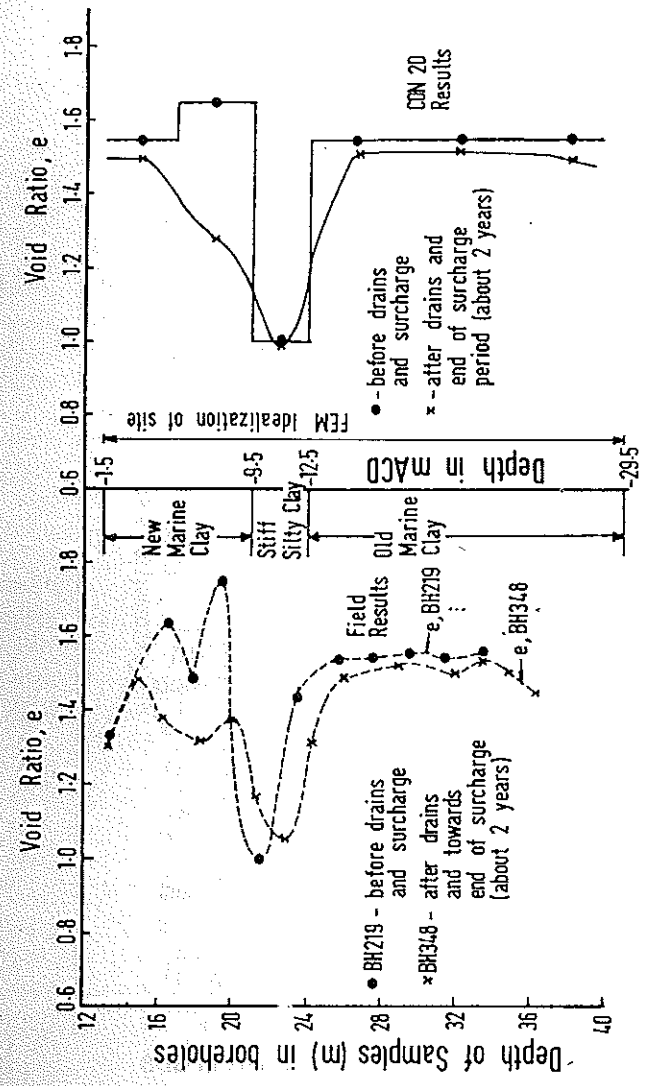Fig. 9 Deep settlements in GD3

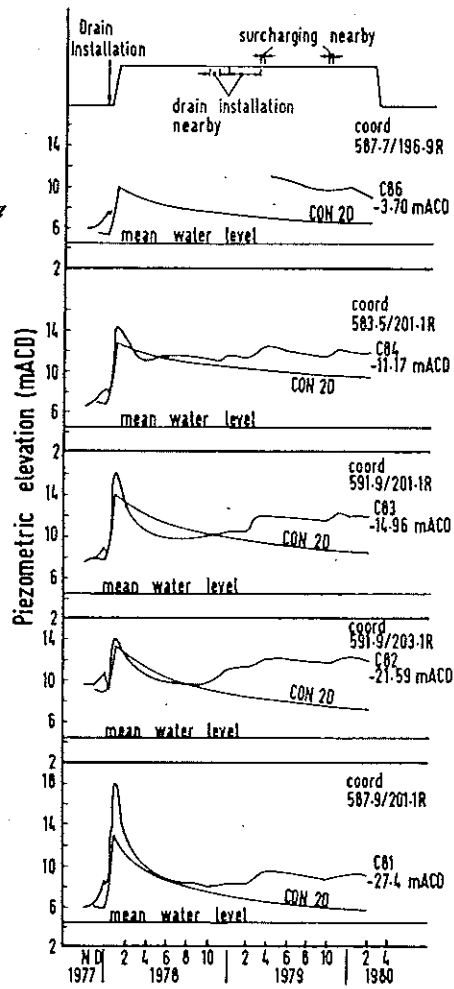Fig. 10 Comparison of void ratio profile between FEM and field measurements

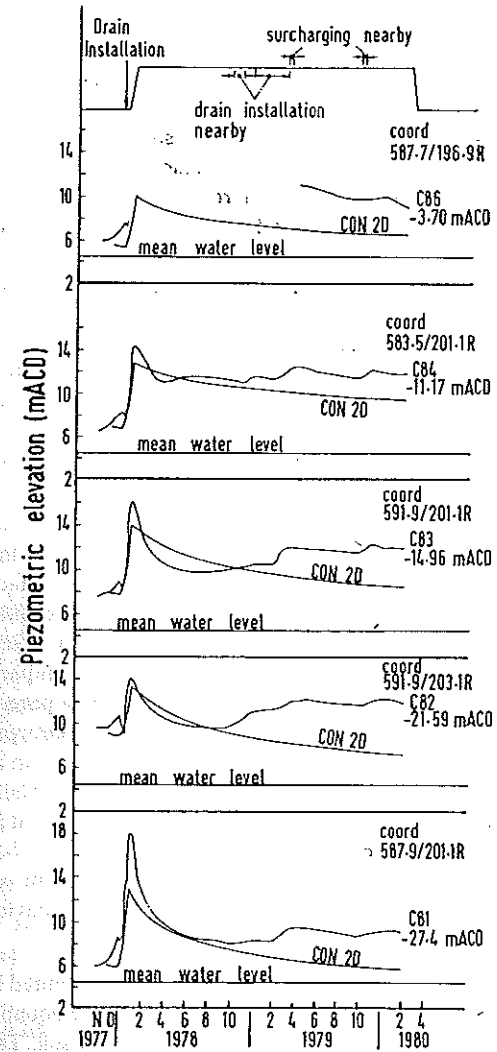Fig. 11   Centreline piezometers in GD3

Fig. 12   Edge of drains piezometers in GD3

drained area precisely as this is a process of consolidation at a point as discussed by Karunaratne et al., (1989).

Away from the centre of the drained zone, pore pressure predictions are better as shown in Fig.12 for piezometers at the edge of GD3. Except for C92, the predictions of the pore pressure rise upon surcharge and subsequent dissipation agrees well with field observations. Predictions diverge from field results where pore pressure stagnation (lack of response) and generation occurred, probably due to nearby excavation (drainage) and backfilling activities.

The pore pressure variations with distance from the taxiway (GD3) centreline at different elevations 18 months after surcharge application are shown in Fig.13. The field results showed that after 18 months of surcharge, the excess pore pressure within the drained zone was 40 to 60kPa. The excess pore pressure increased to around 63 to 80kPa under the surcharge overwidth just beyond the drained zone and fell to a value of 20kPa about 20m beyond the toe of the surcharge. The FEM predictions showed the same form as the field observations, illustrating the spread of pore pressure from the clay under the surcharge overwidth into the drained zone and also the back pressure from the clay under the reclamation beyond the surcharge embankment. In contrast with the construction of an embankment on a normally consolidated clay deposit where pore pressure dissipates with flow along the vertical drains and laterally into adjacent areas, the pore pressure in the untreated clay is still high due to underconsolidation. Since the treated area is small in comparison with the untreated area in the whole reclamation, the lowest stable pore pressure level within the drained area is controlled by the prevailing pore pressure in the untreated area.

CONCLUSIONS

(1) A 2D plane strain finite element model with an elasto-plastic soil constitutive model has been used to describe reasonably well the behaviour of recently reclaimed land treated with drains and surcharge.

(2) Vertical drains in a 2D plane strain analysis can be accounted for by using an enhanced equivalent vertical permeability obtained by equating the surface settlement of the real soil with that of the equivalent soil. The method will allow accurate estimates of settlements and approximate estimates of pore pressures in the treated area.

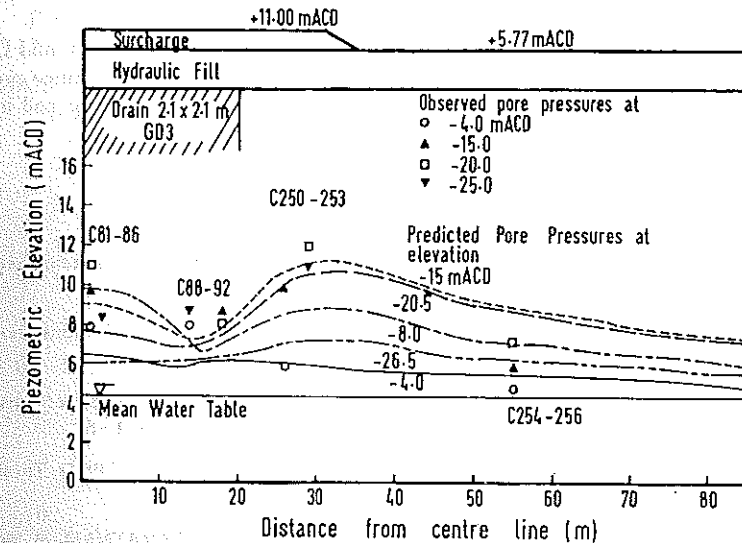Fig. 13   Predicted and observed pore pressures in GD3 (18 months after surcharge)

(3) The soil parameters used in the analysis must be carefully calibrated based on field and laboratory measurements. Well defined boundary and initial conditions must be determined from site investigations and variations of soil compressibilities and permeabilities with the consolidation process must be accounted for by a rational constitutive model before reasonable predictions can be made.

(4) The influence of construction activities in the neighborhood such as drain installations and fill surcharging, can greatly complicate the pore pressure response of a test site making correct interpretations and predictions difficult.

(5) Design and analysis of soil improvement works for recently reclaimed fills using drains and surcharge must account for the back pressure effect due to underconsolidation of the reclaimed land. The back pressure effect can be analysed by a proper 2D analysis of the reclamation sites.

ACKNOWLEDGEMENTS

REFERENCES

ALPAN, I. (1967). "The empirical evaluation of K_o and K_{or}." *Soils and Foundations,* Vol.7, No.1, pp. 31–40.

BARRON, R.A. (1948). "Consolidation of fine grained soils by drain wells." *Transactions of ASCE, Paper No.2340,* Vol.113, pp. 718–742.

CARILLO, N. (1942). "Simple two and three dimensional cases in the theory of consolidation of soils." *Journal of Mathematics and Physics,* Vol.21, pp. 1–5.

CHOA, V. (1986). *"Consolidation of marine clay under reclamation fills."* Ph.D. Thesis, National University of Singapore.

CHOA, V., KARUNARATNE, G.P., RAMASWAMY, S.D., VIJIARATNAM, A. and LEE, S.L. (1979). "Pilot test for soil stabilization at Changi Airport." *Proceedings 7th Asian Regional Conference on Soil Mechanics and Foundation Engineering, Singapore,* Vol.1, pp. 141–144.

CHOA, V., VIJIARATNAM, A., KARUNARATNE, G.P., RAMASWAMY, S.D. and LEE, S.L. (1979). "Consolidation of Changi marine clay of Singapore using flexible drains." *Proceedings 7th European Regional Conference on Soil Mechanics and Foundation Engineering,* Brighton, Vol.3, pp. 29–36.

CHOA, V., KARUNARATNE, G.P., RAMASWAMY, S.D., VIJIARATNAM, A. and LEE, S.L. (1981): "Drain performance in Changi marine clay." *Proceedings 10th International Conference on Soil Mechanics and Foundation Engineering, Stockholm,* Vol.3, pp. 623–626.

DUNCAN, J.M., D'ORAZIO, T.B., CHANG, C.S., WONG, K.S. AND NAMIQ, L.I. (1981). *"CON2D a finite element computer program for analysis of consolidation."* U.C. Berkeley Report, UCB/CHT/81–01.

DUNCAN, J.M. and D'ORAZIO, T.B. (1984). "Stability of steel oil storage tanks." *ASCE Journal of Geotechnical Engineering,* Vol.110, No.9, pp. 1219–1238.

HANSBO, S. (1981). "Consolidation of fine-grained soil by means of cardboard wicks." *Proceedings of 10th Int. Conf. on SMFE,* Stockholm, Vol.3, pp. 677–682.

KARUNARATNE, G.P., TAN, S.A., LEE, S.L. and CHOA, V. (1989). "Analysis of *flexible drains in Changi reclamation." Canadian Geotechnical Journal,* Vol. 26, No.3, pp. 401–417.

TAN, S.A., LEE, S.L., KARUNARATNE, G.P. and CHOA, V. (1987). "Design of drains and surcharge in reclamations." *Soils and Foundations,* Vol.27, No.4, pp. 89–98.